



Performance and characterisation of CsI:Tl thin films for X-ray imaging application

E. A. Kozyrev, K. E. Kuper, A. G. Lemzyakov, A. V. Petrozhitskiy, and A. S. Popov

Budker Institute of Nuclear Physics
Novosibirsk State University
e.a.kozyrev@inp.nsk.su



Novosibirsk, July 7, 2016

Plan

1. Introduction

2. Thin CsI:Tl scintillator films

- the fabrication of scintillator films
- crystalline properties
- MTF, light output
- additional treatments

3. CsI:Tl films for X-ray

- Imaging
- Tomography
- Topography and etc.

4. Conclusion

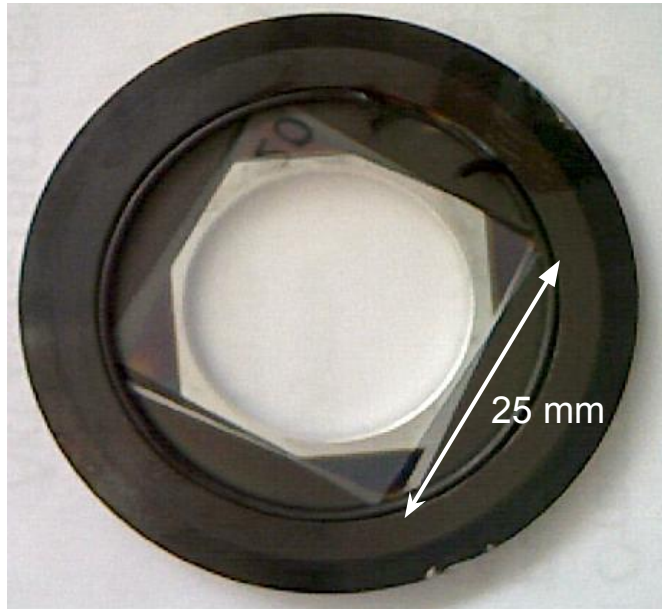
1. Introduction

CsI(Tl) scintillator films are widely applied as the conversion screens for the indirect X-ray imaging. The CsI(Tl) is characterized by one of the highest conversion efficiencies of any known scintillator.

+ Microstructure inside volume decreases the lateral spreading of scintillating light.

Due to a wide range of applications (crystallography, microtomography, digital radiography and etc.) the development of preparation methods is relevant.

2. Thin CsI:Tl films: performance and properties



CsI:Tl scintillation films were manufactured by the thermal deposition method.

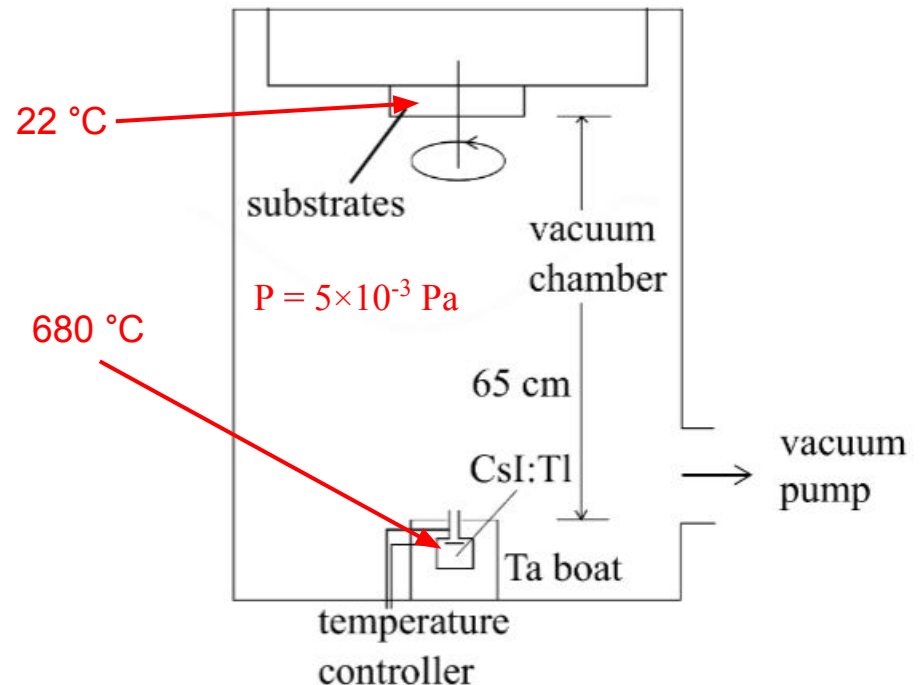
Substrates: glass (150 mkm),
Mylar (DuPont, 2.9 mkm)
saphir (800 mkm)

Thickness of CsI:Tl films: 2-10 mkm

The average velocity of deposition of CsI:Tl
 $= 17 \text{ \AA}/\text{sec}$.

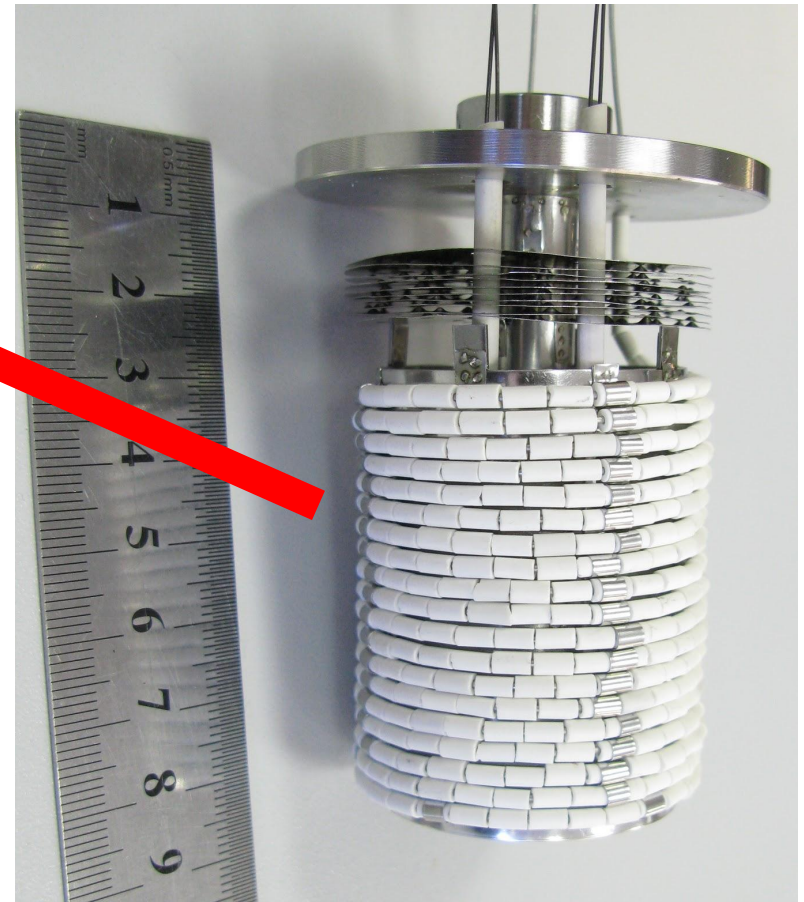
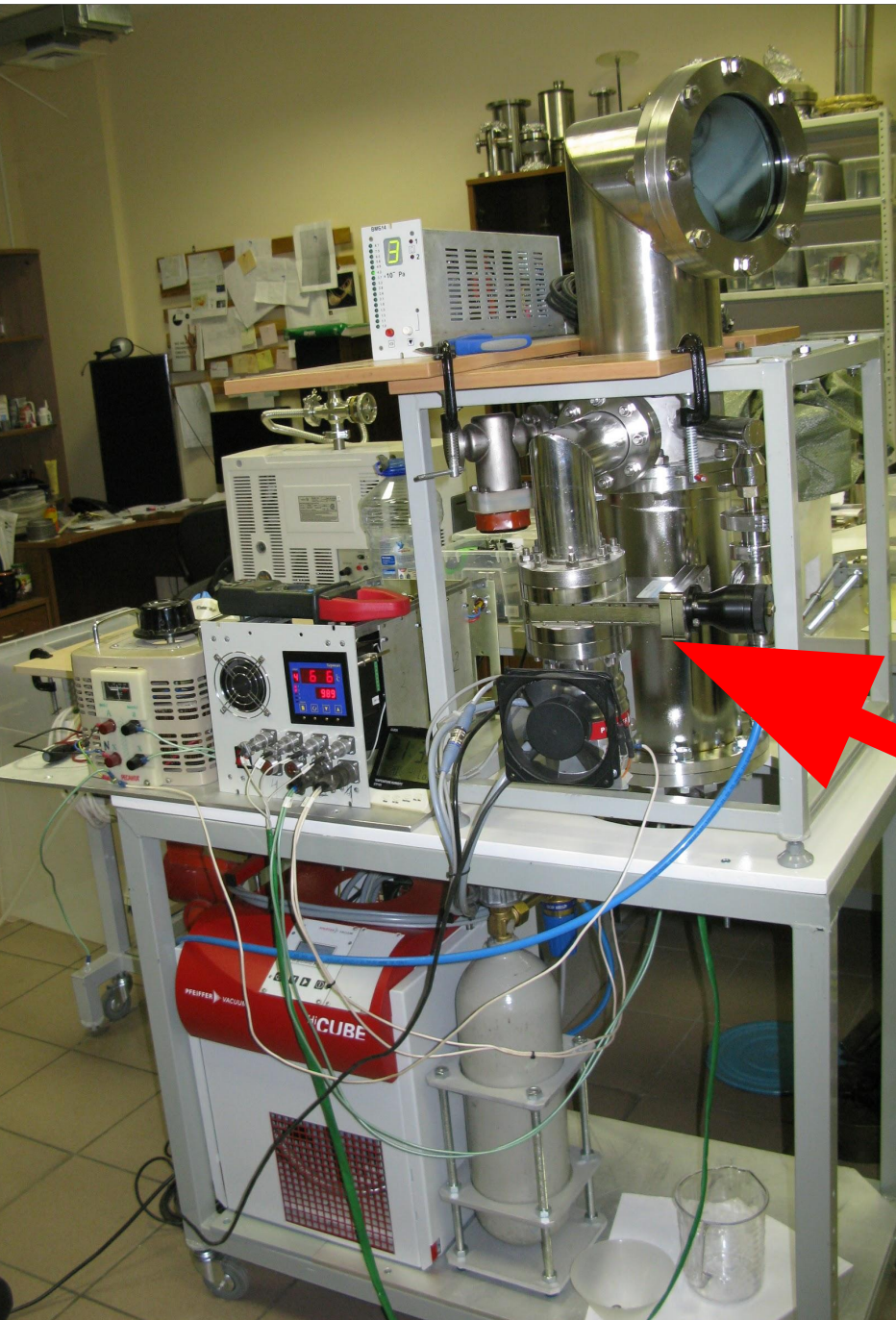
The scintillator volume is characterized by
grain structure.

The grain structure depends on the type of
used substrate and on the velocity of CsI:Tl
deposition.

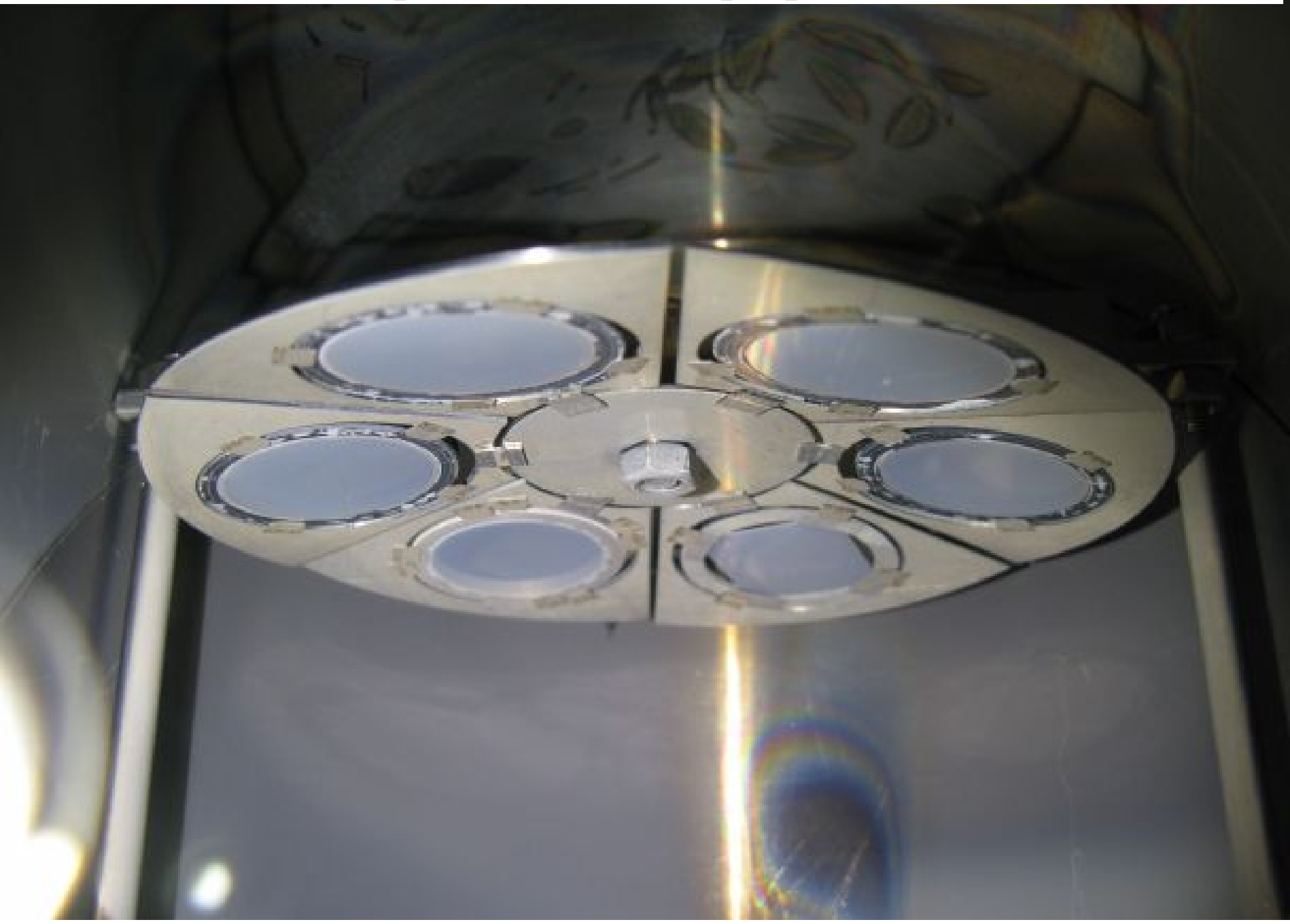


Schematic of the thermal evaporation setting

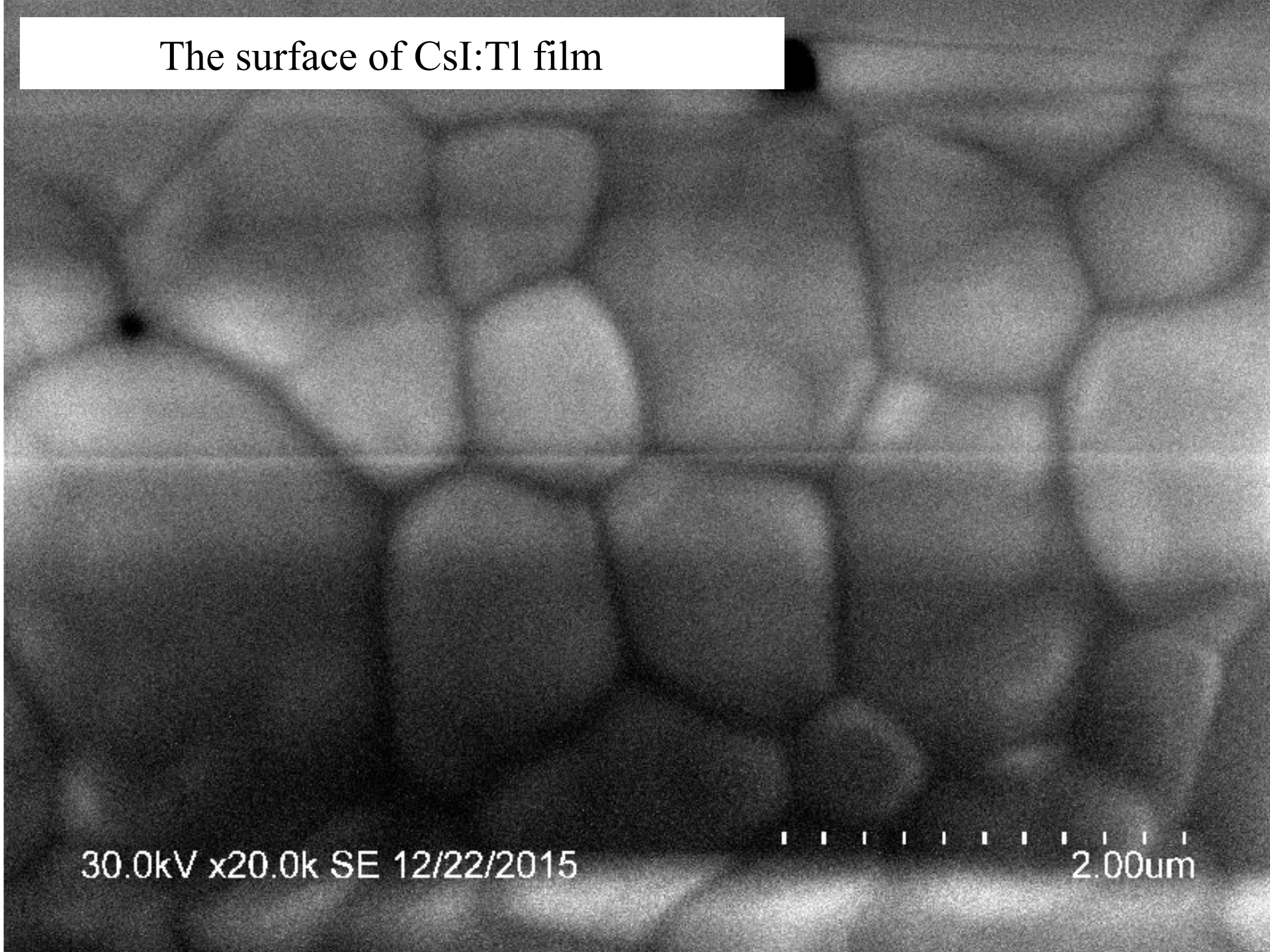
2. Thin CsI:Tl films: performance and properties



2. Thin CsI:Tl films: performance and properties



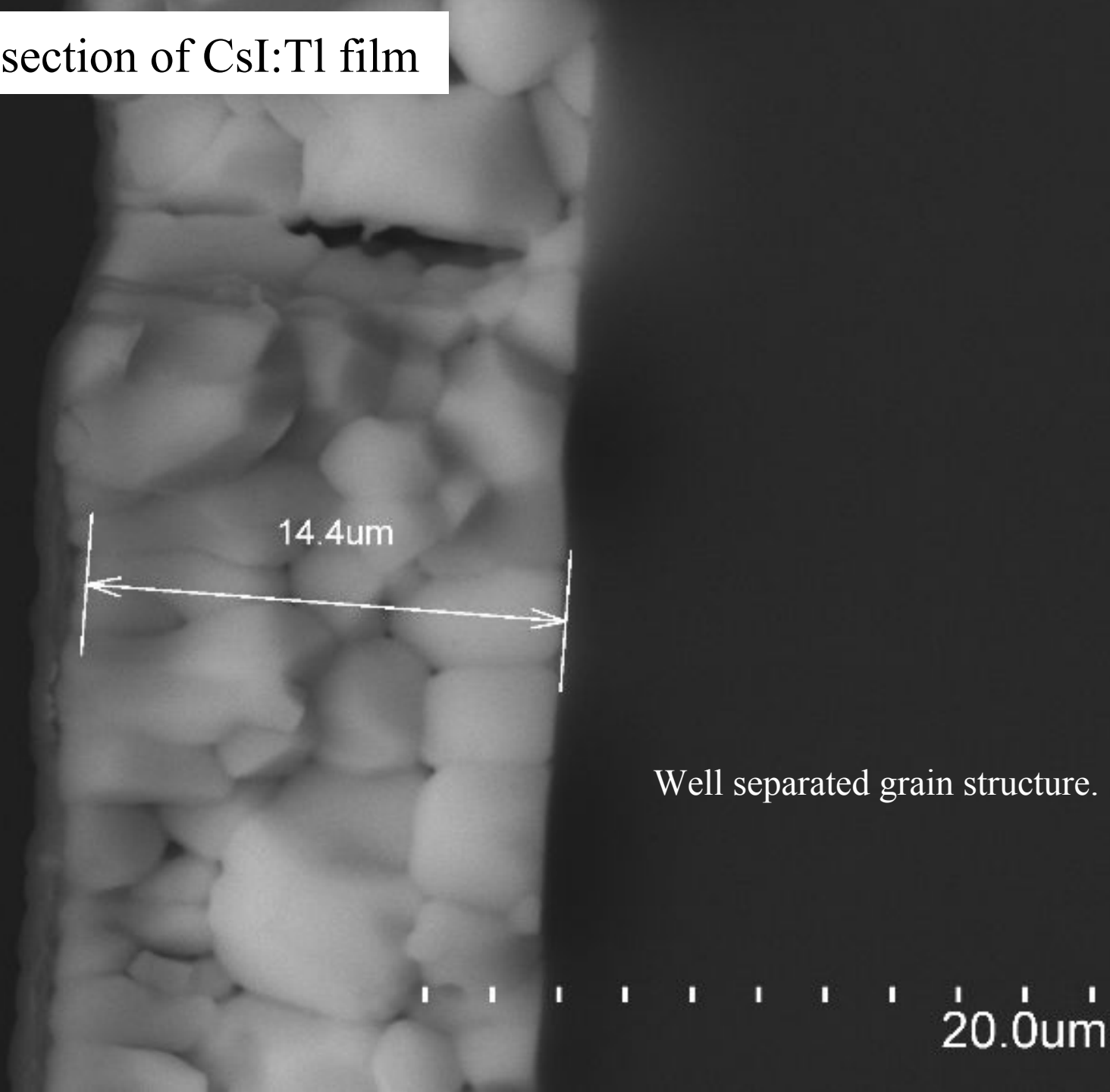
The surface of CsI:Tl film



30.0kV x20.0k SE 12/22/2015

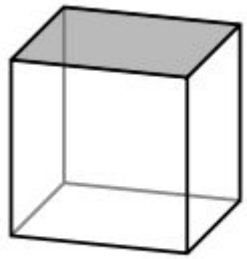
2.00um

The cross section of CsI:Tl film

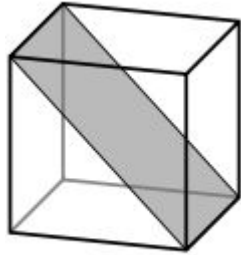


2. Thin CsI:Tl films: performance and properties

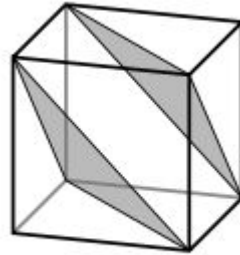
The CsI:Tl orientation was measured using electron backscattering diffraction



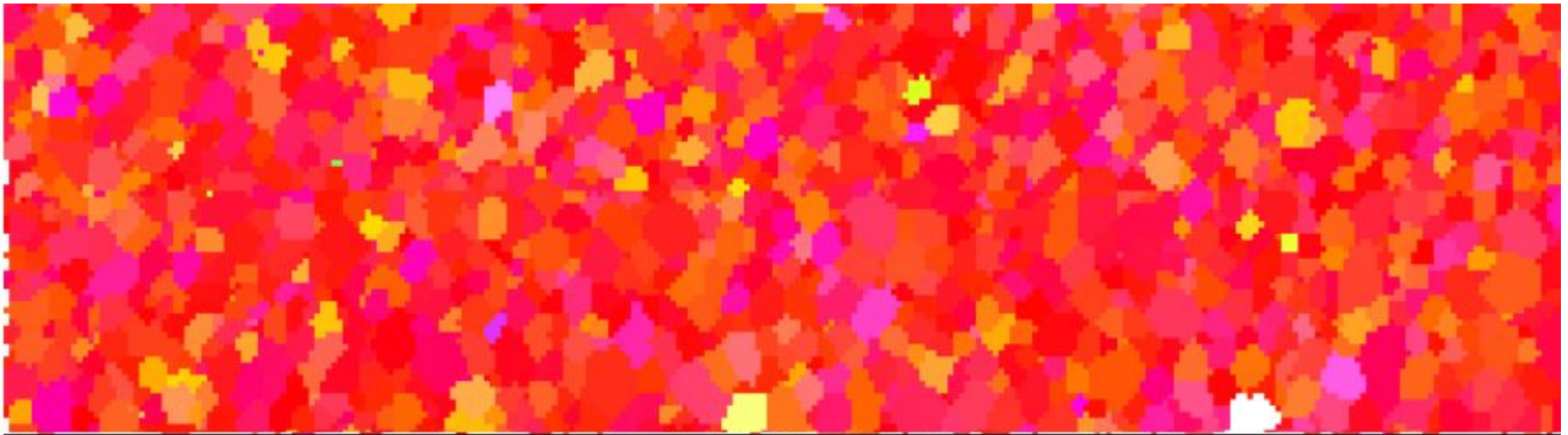
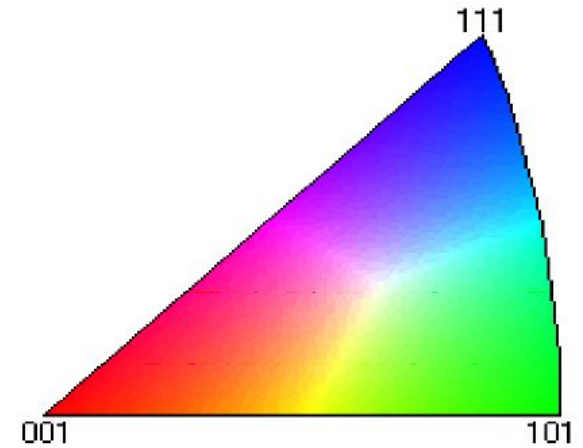
(001)



(101)



(111)

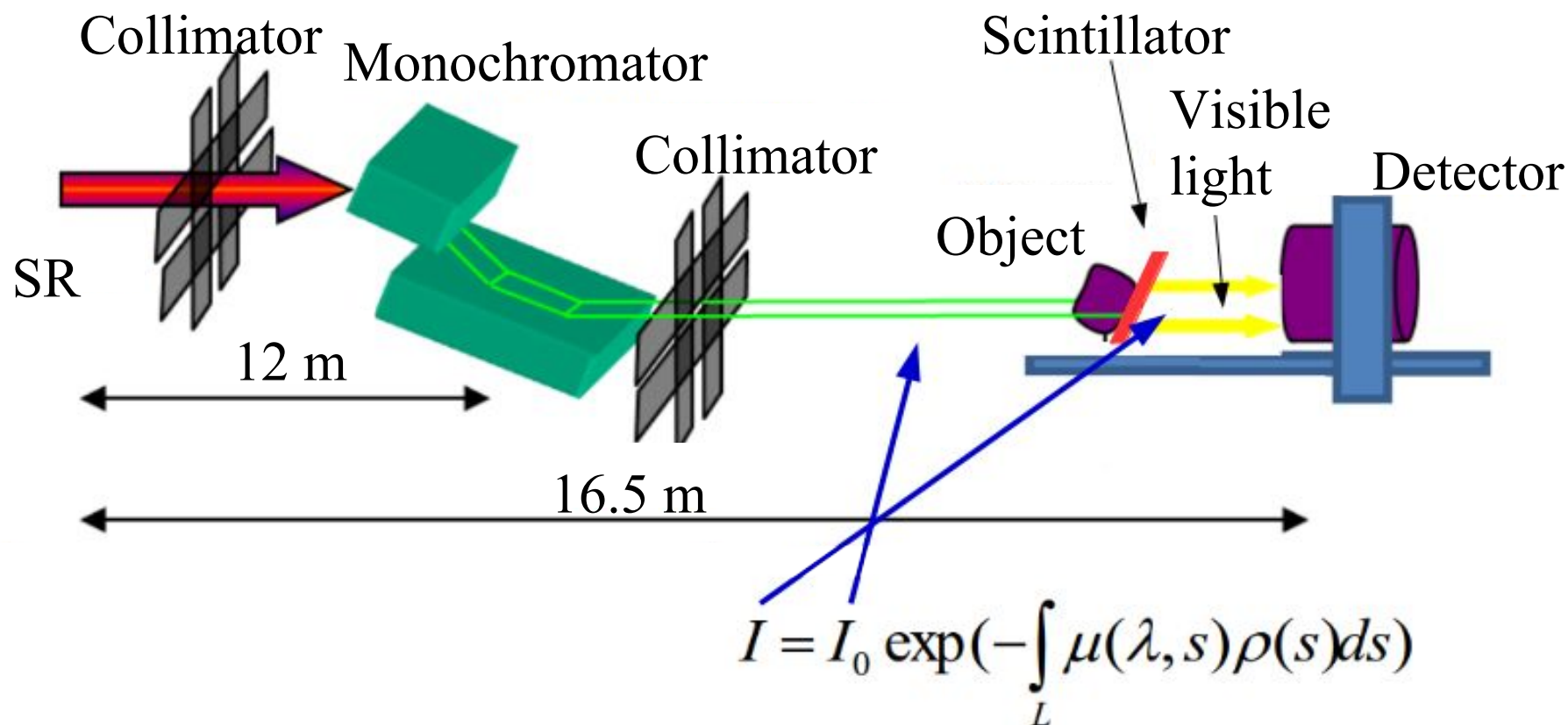


100 μm

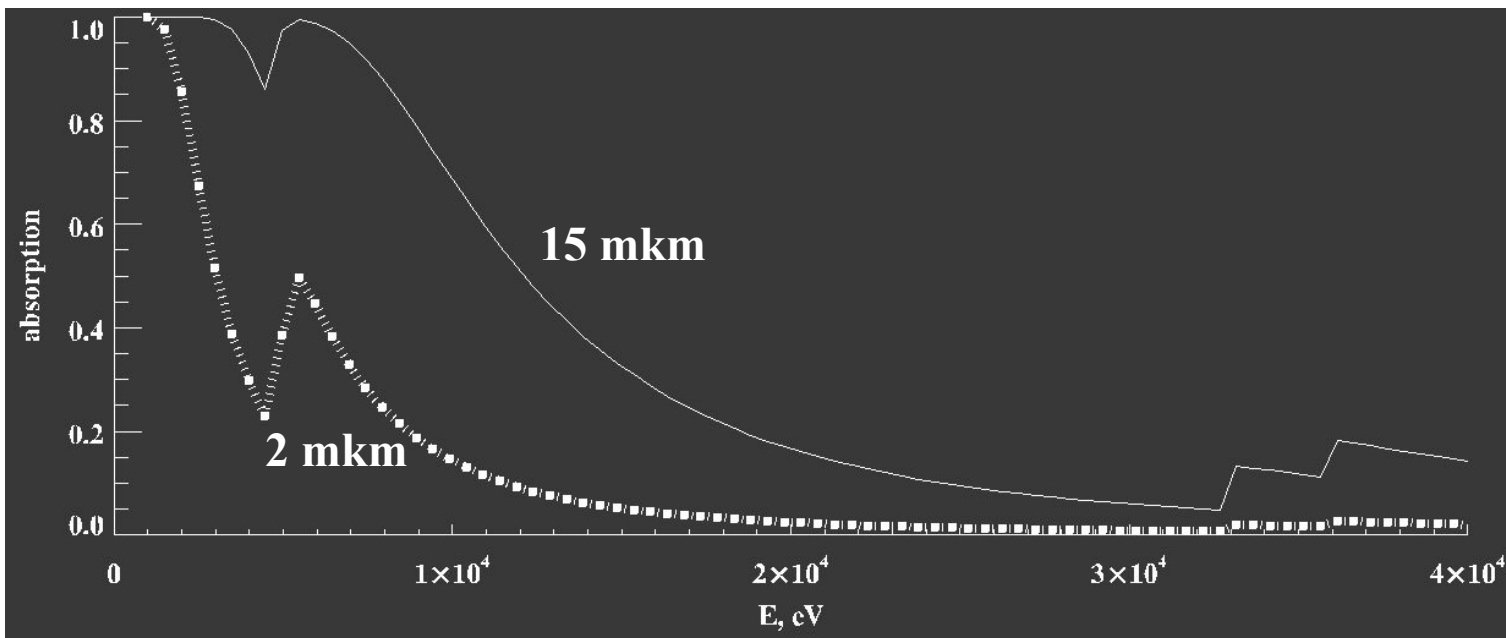
2. Thin CsI:Tl films: performance and properties

The CsI:Tl films was performed with different

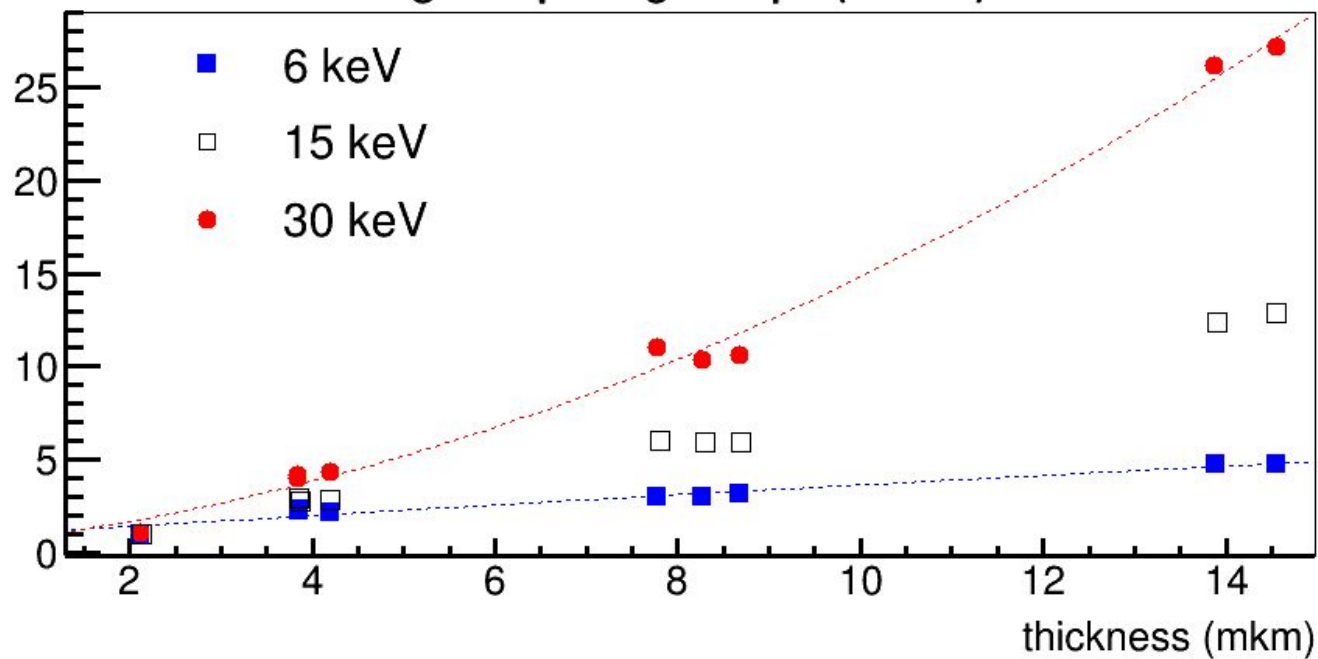
- thicknesses
- substrates
- evaporation velocities
- after evaporation treatments



2. Thin CsI:Tl films: performance and properties

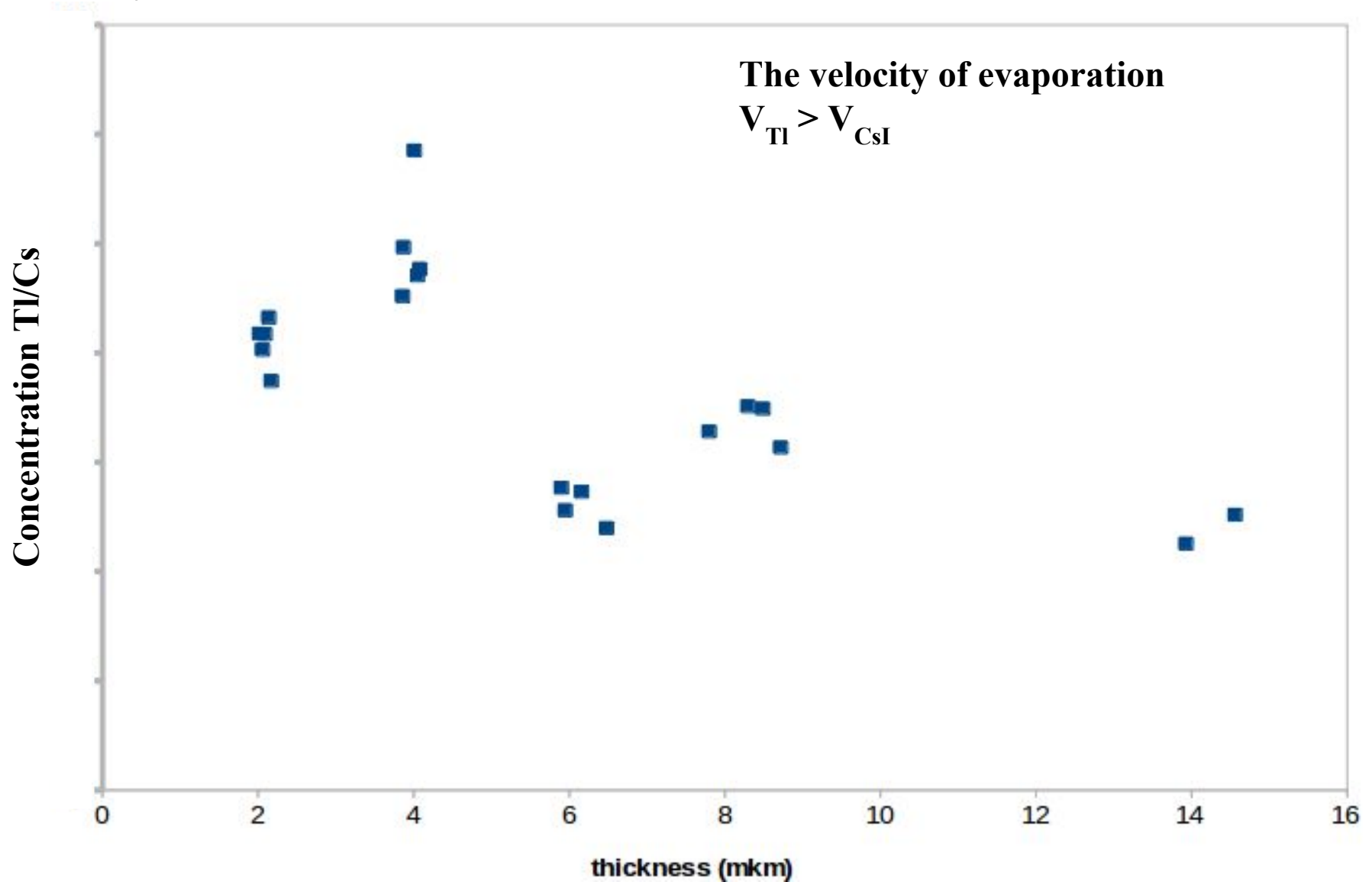


lightoutput /lightoutput(2 mkm)



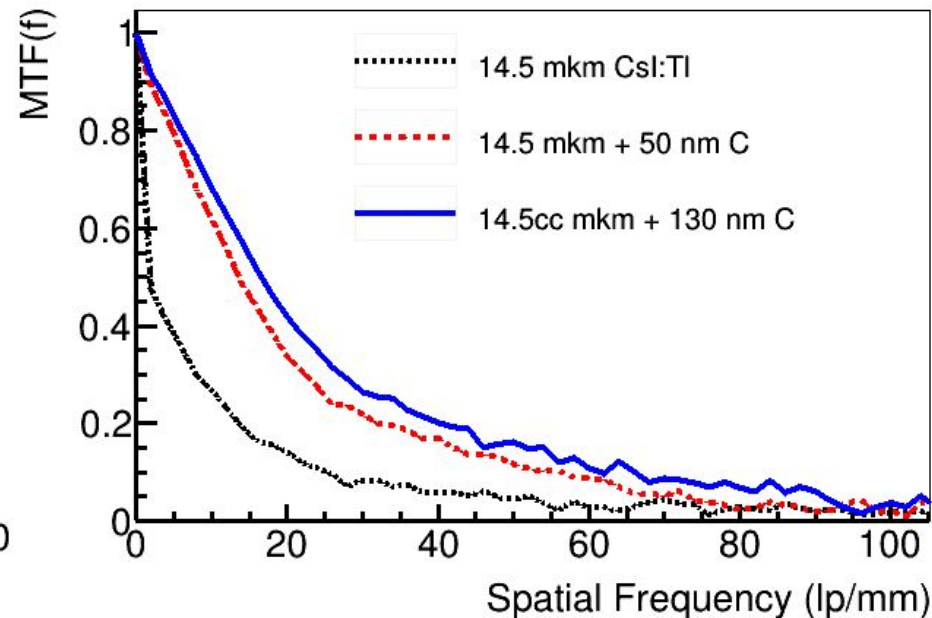
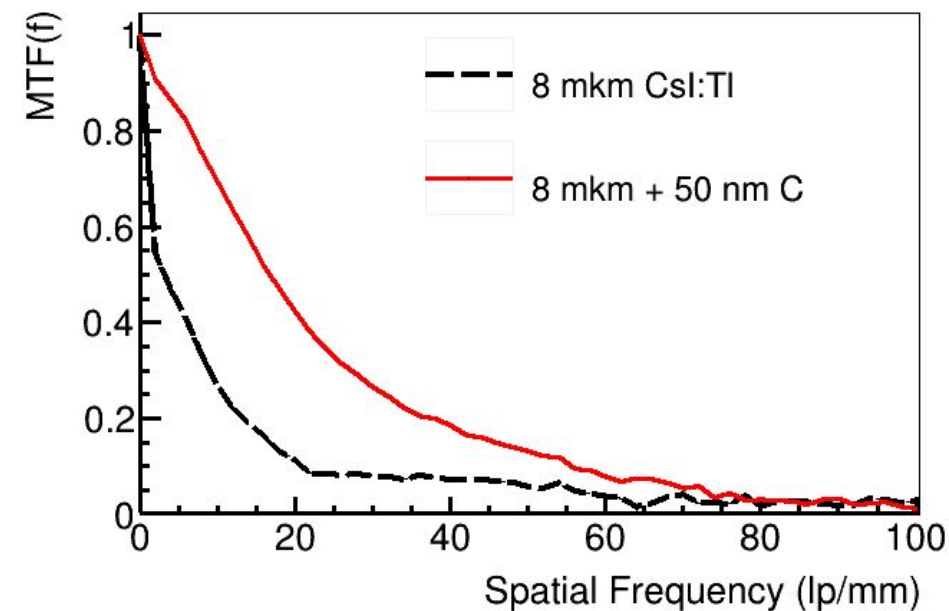
2. Thin CsI:Tl films: performance and properties

An X-ray fluorescence analysis allow to measure the concentration of Tl relatively to Cs:

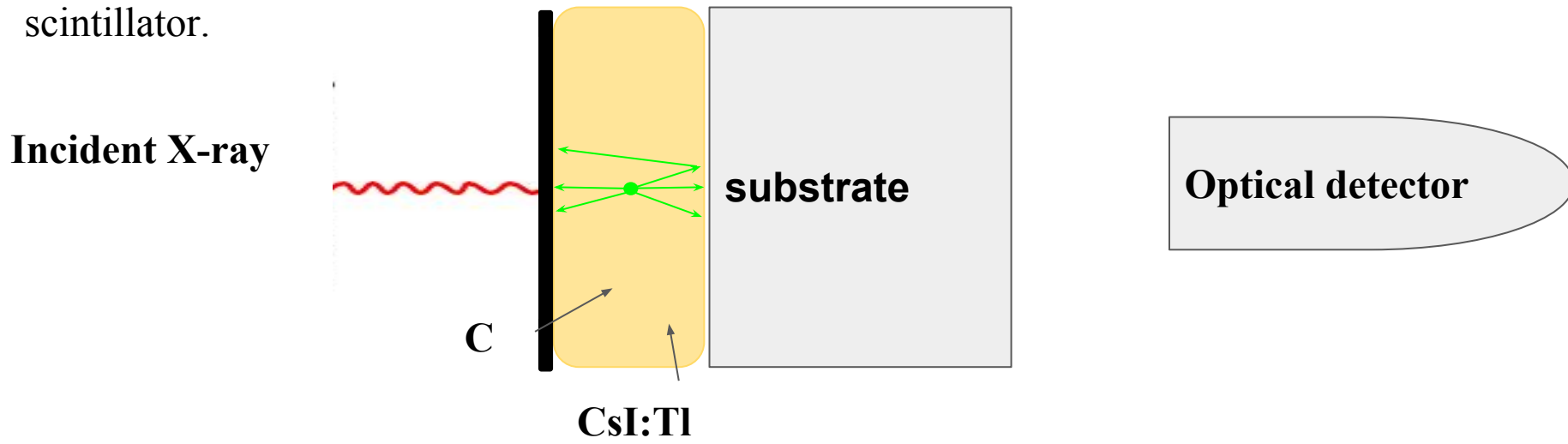


2. Thin CsI:Tl films: performance and properties (MTF)

Additional carbon layer was performed by magnetron deposition method. Required carbon thickness is about 150 nm. Light output decreases by 2-3 times.



The additional carbon layer removes the multiple scattering of visible photons inside scintillator.



2. Thin CsI:Tl films: performance and properties

Mylar substrate

30.0kV x4.50k SE 11/23/2015

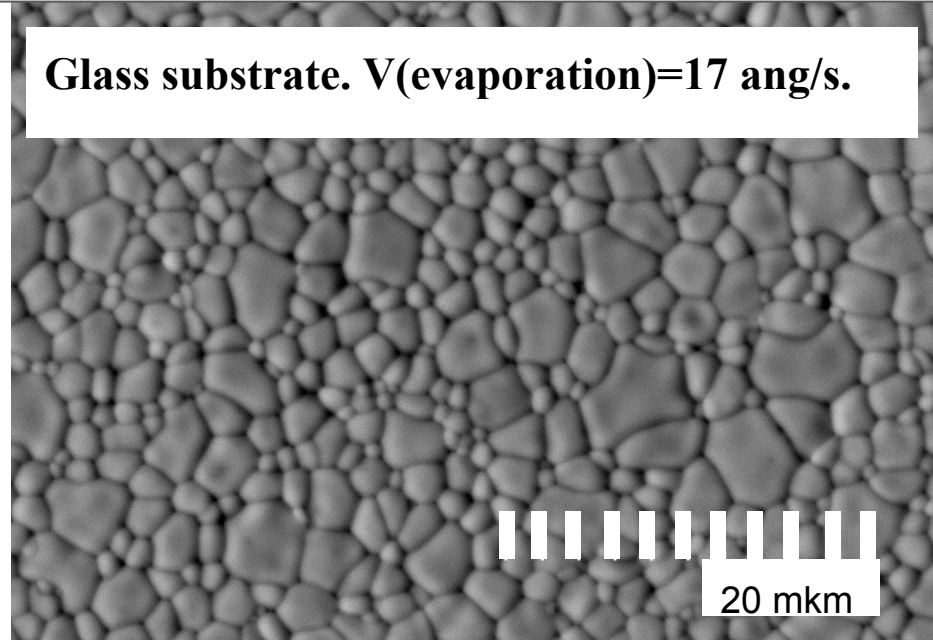


10 mkm

Glass substrate. $V(\text{evaporation})=17 \text{ ang/s}$.

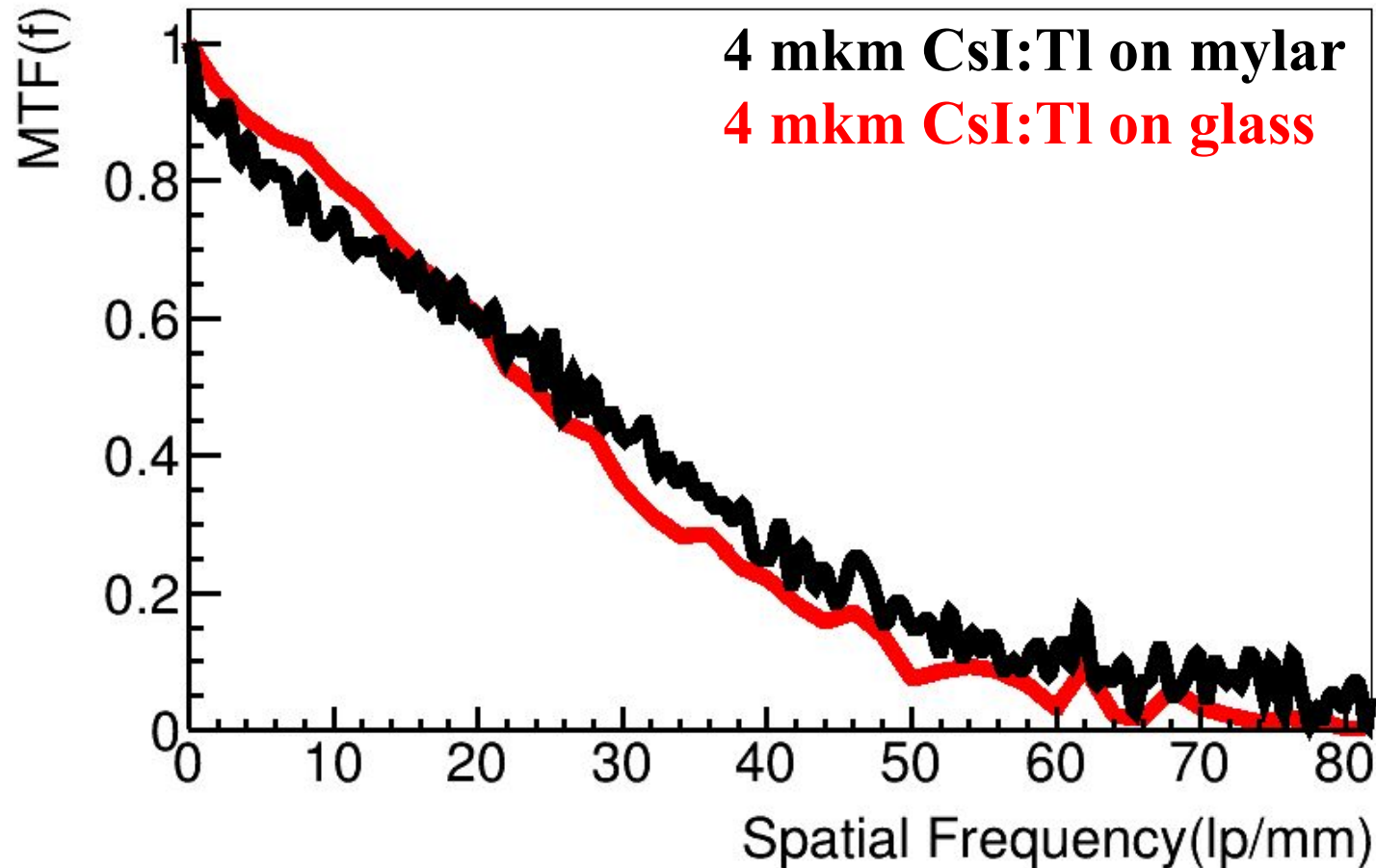


20 mkm



2. Thin CsI:Tl films: performance and properties (MTF)

The size of grains in thin scintillator is not strongly correlated with spatial resolution.



Problem!!! During carbon deposition on scintillator with mylar substrate, the heating of mylar leads to the evaporation of 90% thallium.

2. Thin CsI:Tl films: performance and properties

Mylar substrate

30.0kV x4.50k SE 11/23/2015



Glass substrate. $V(\text{evaporation})=17$ ang/s.



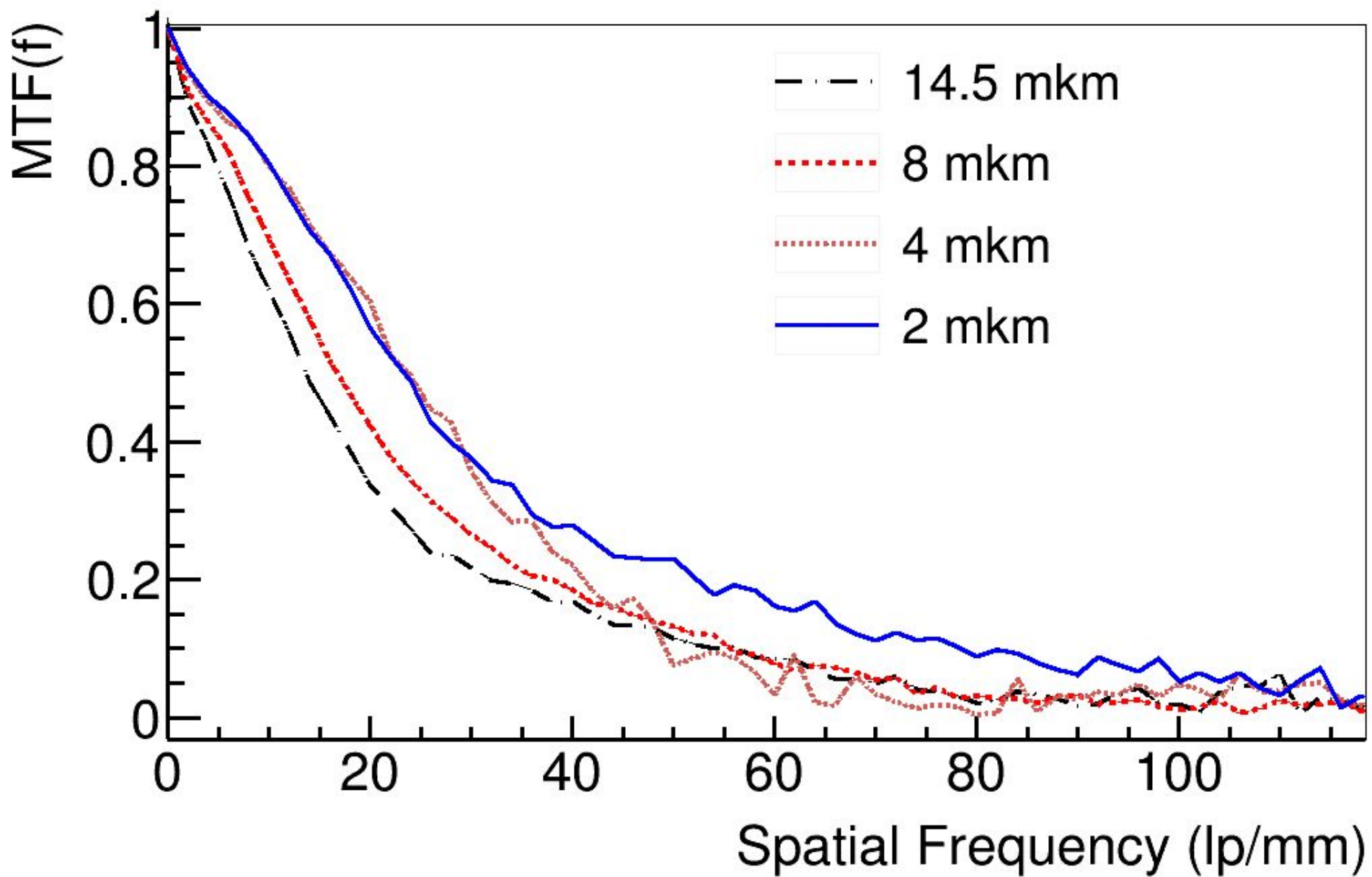
Glass substrate. $V(\text{evaporation})=10$ ang/s.



Glass substrate. $V(\text{evaporation})=25$ ang/s.



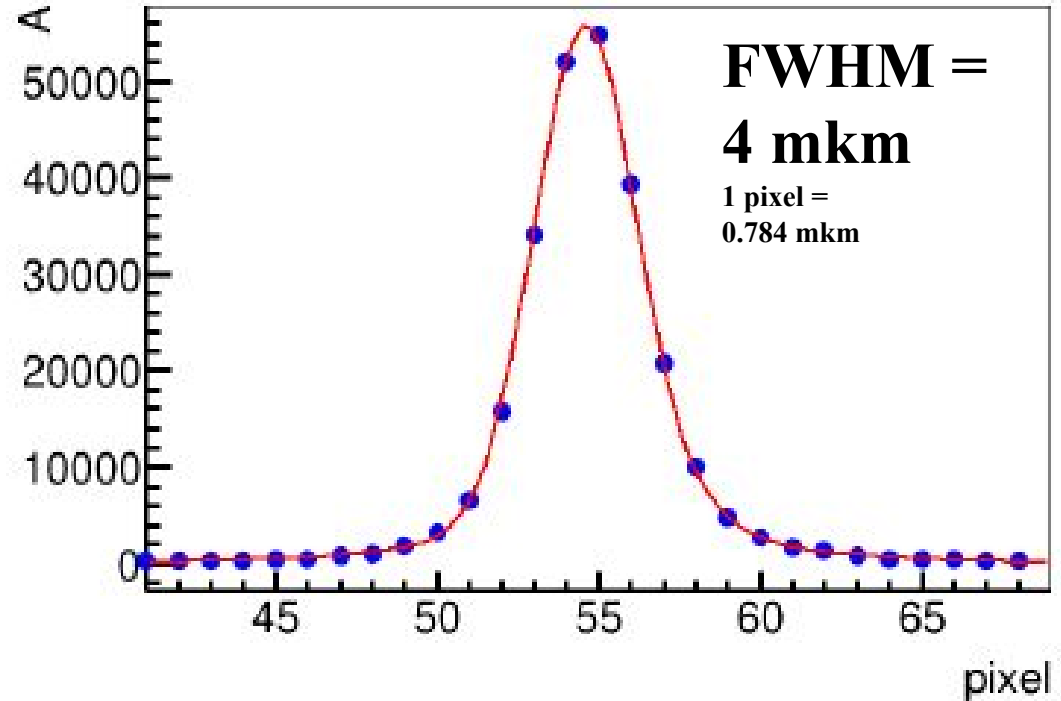
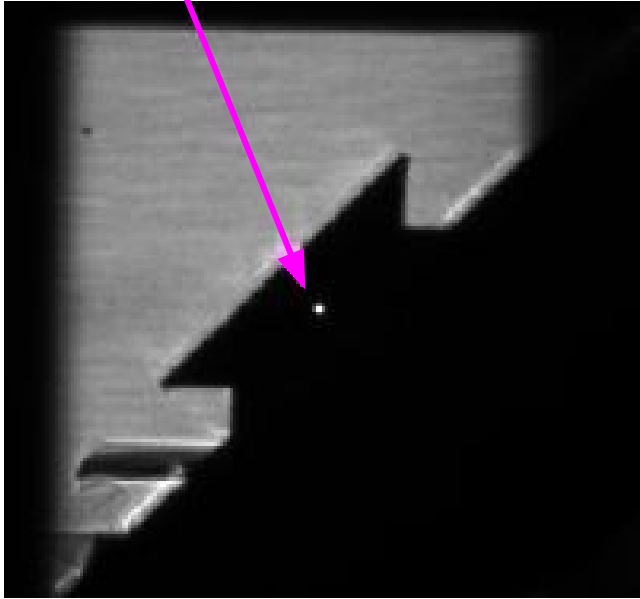
2. Thin CsI:Tl films: performance and properties (MTF)



2. Thin CsI:Tl films: performance and properties (MTF)

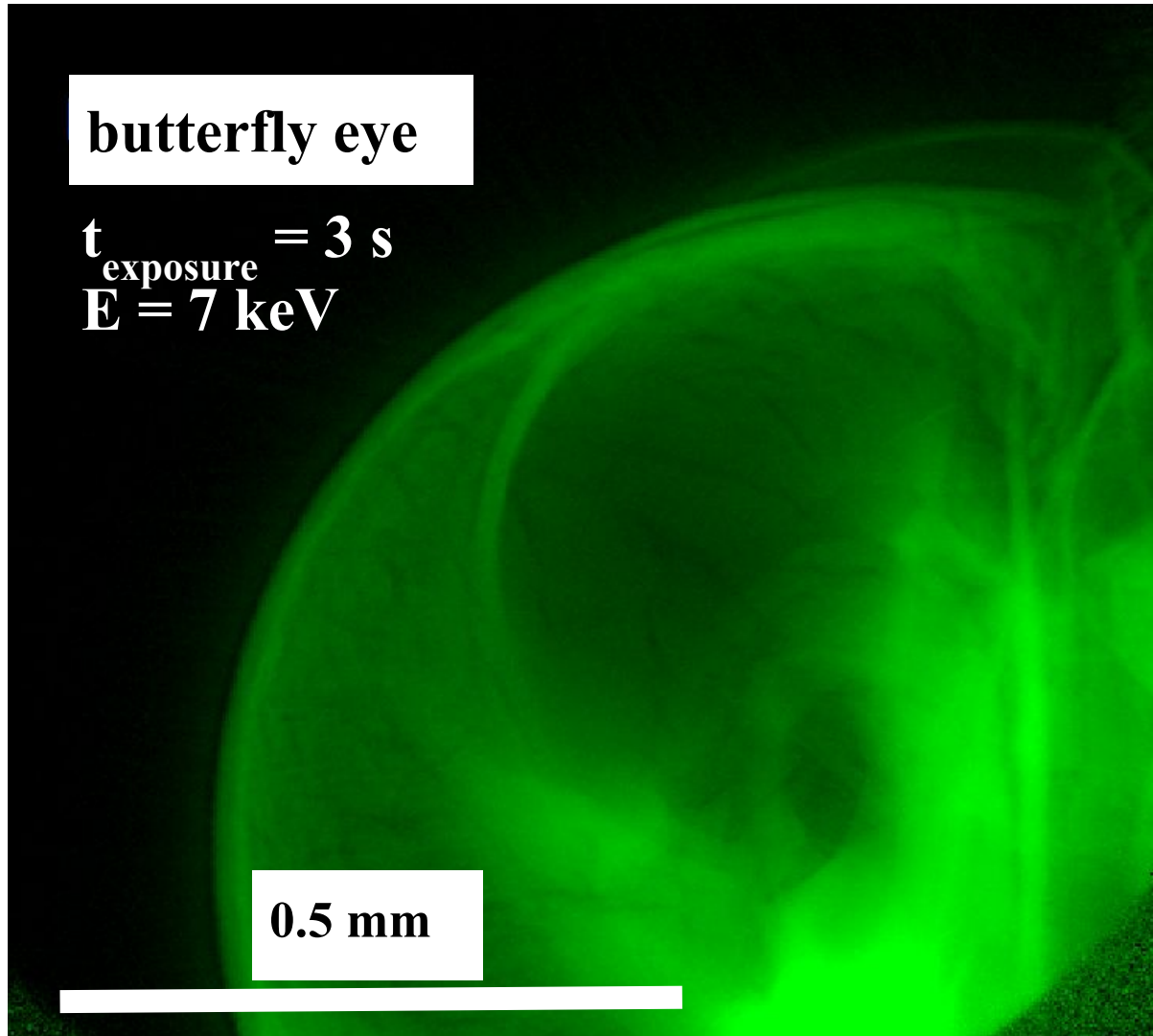
The using of SU-8 refractive compound lens allow to obtain the approach to point spread function.

The focus on scintillator film



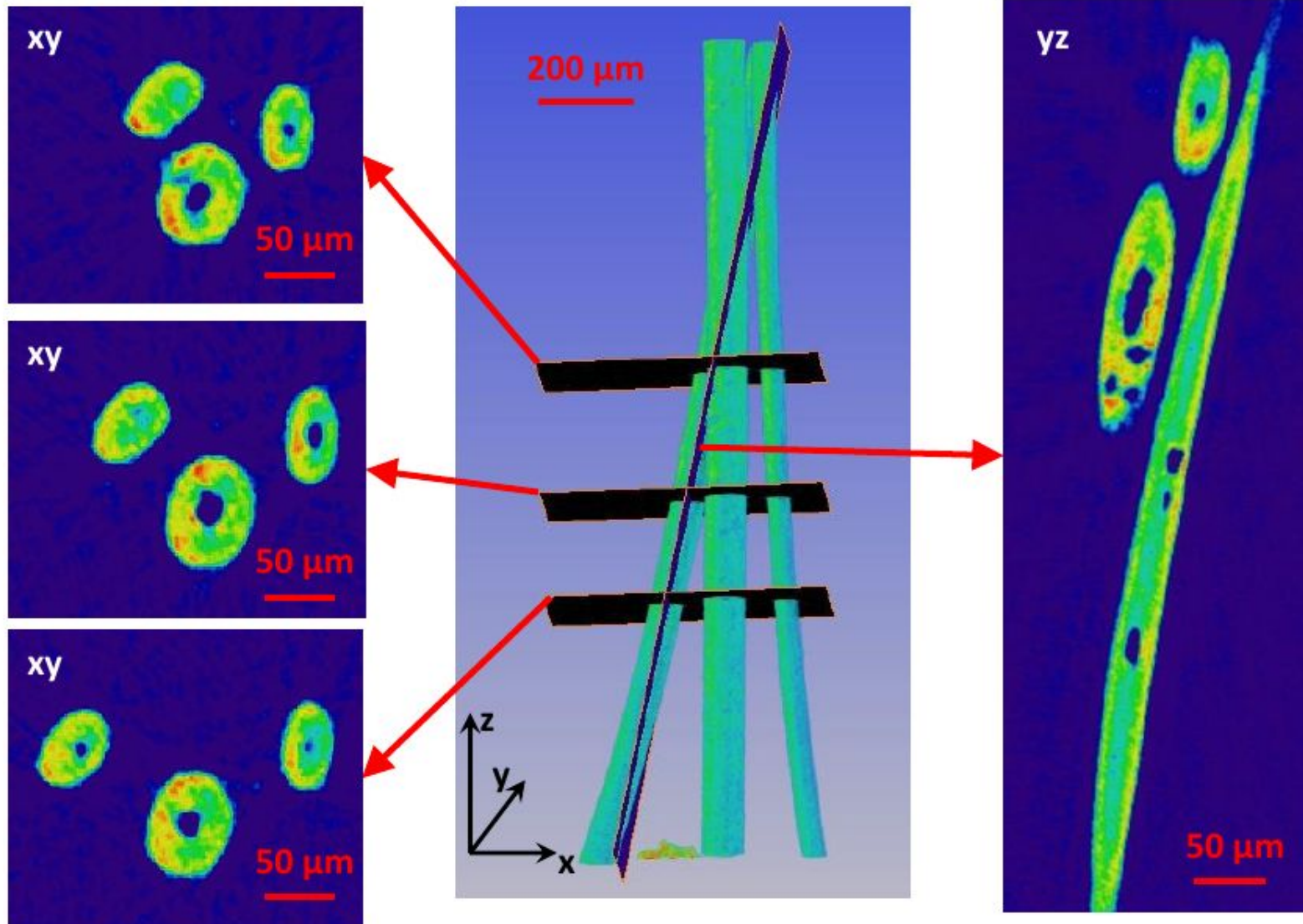
3. CsI:Tl films for X-ray Imaging

Performed CsI:Tl films allow to make radiography in wide X-ray energy region [5-100] keV.



3. CsI:Tl films for X-ray Imaging

3D image of ancient hair from Ak-Alaha tomb (Altai, plateau Ukok). $E = 9$ keV.
A hollow hair is unsuitable for genetic analysis. The goal of the investigation is to find not damaged regions.

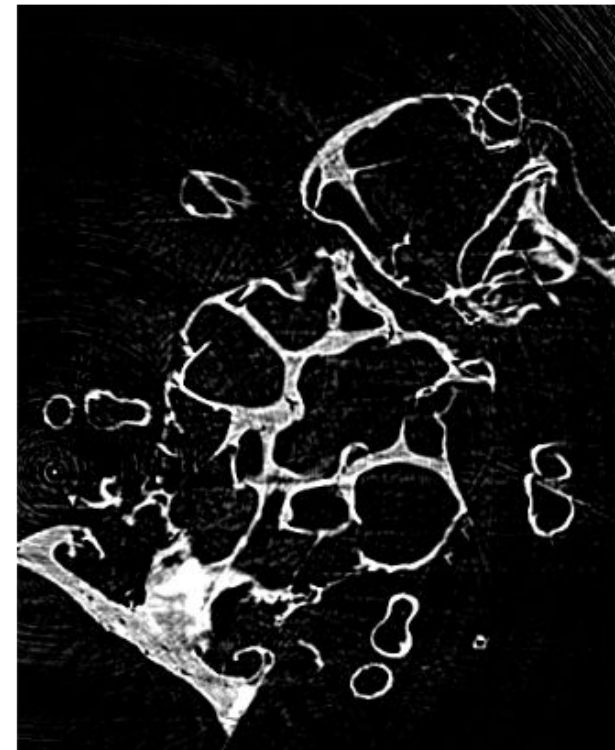


3. CsI:Tl films for X-ray Imaging

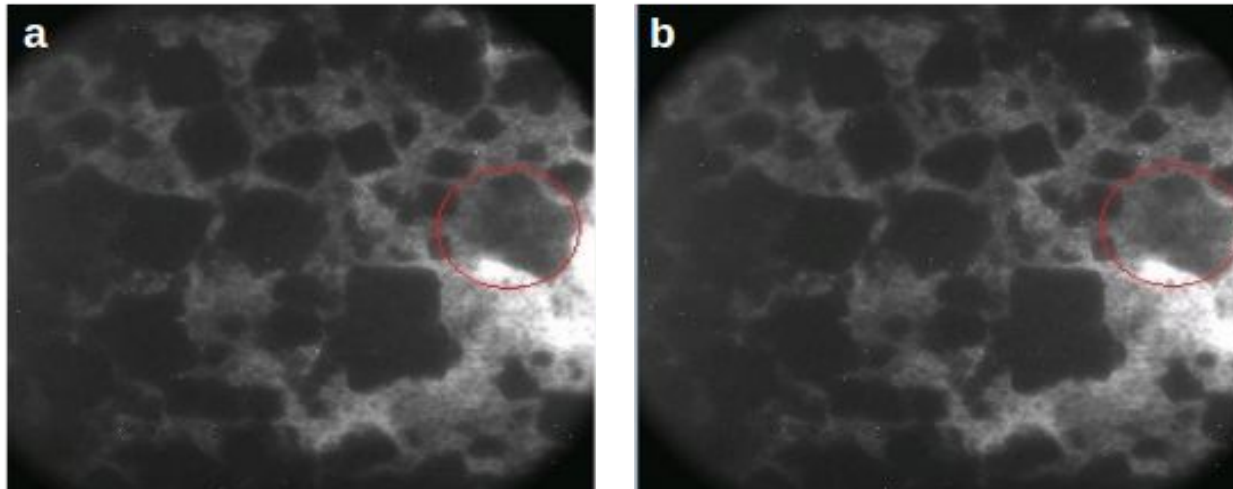


3D tomography of drosophila. $E = 9 \text{ keV}$.

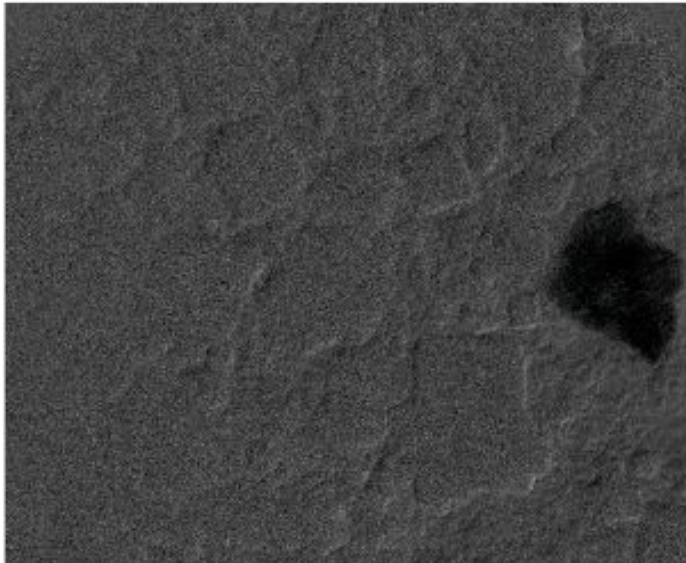
$N_{\text{rotation}} = 180$. $T_{\text{exposure}} = 3 \text{ s}$.



3. CsI:Tl films for X-ray Imaging



The imaging of multicomponent high-energy fuel with X-ray energies $E = 6.537$ keV (a) and $E = 6$ keV (b)



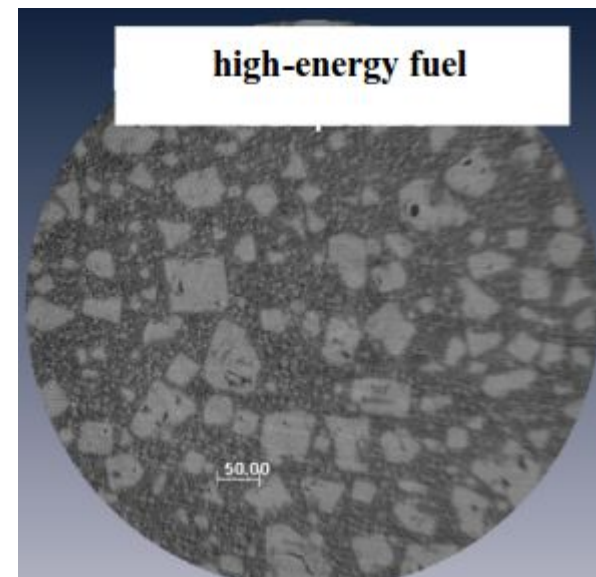
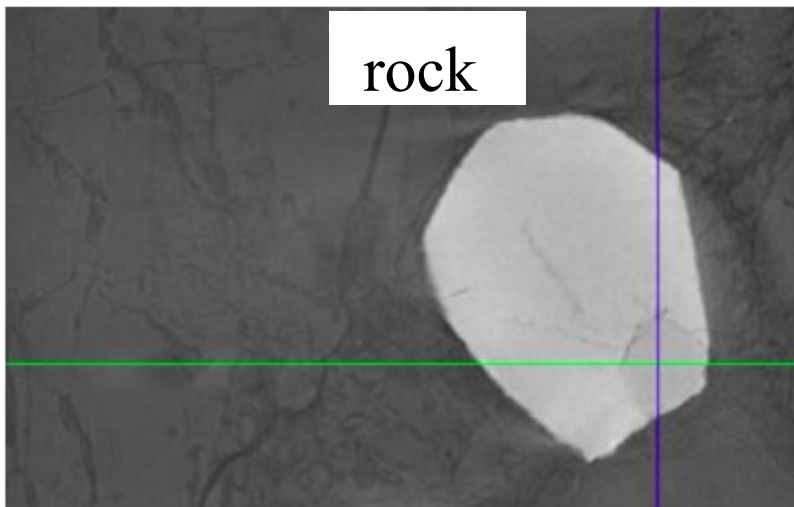
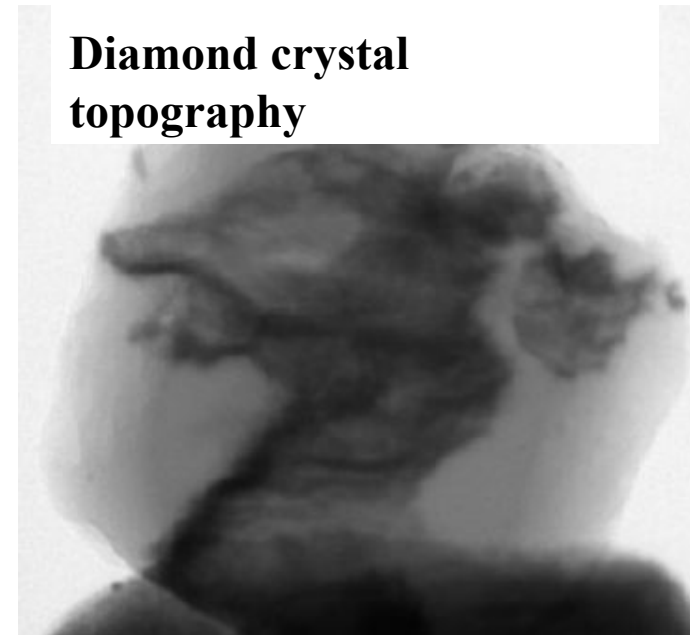
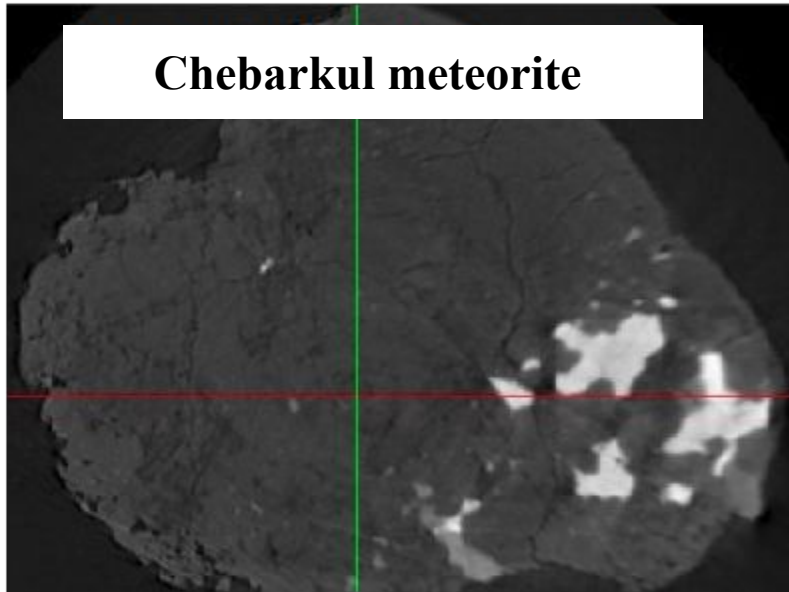
The energy of Mn K-edge $E_{\text{K}}^{\text{Mn}} = 6.29$ keV

The contrast area corresponds to Mn element.

The difference Fig.a - Fig.b.

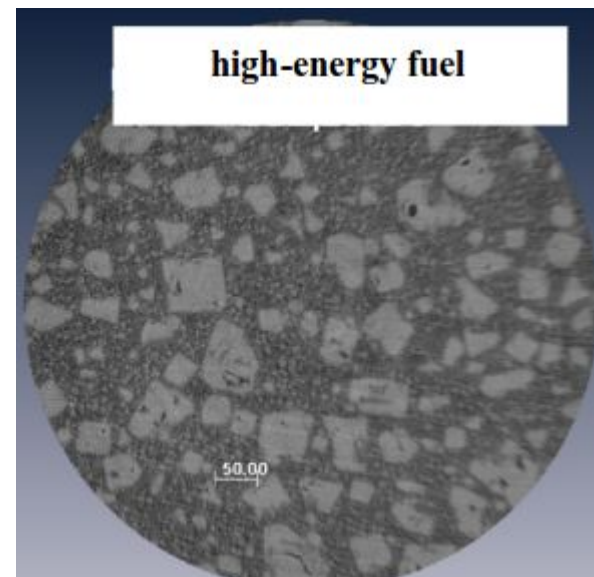
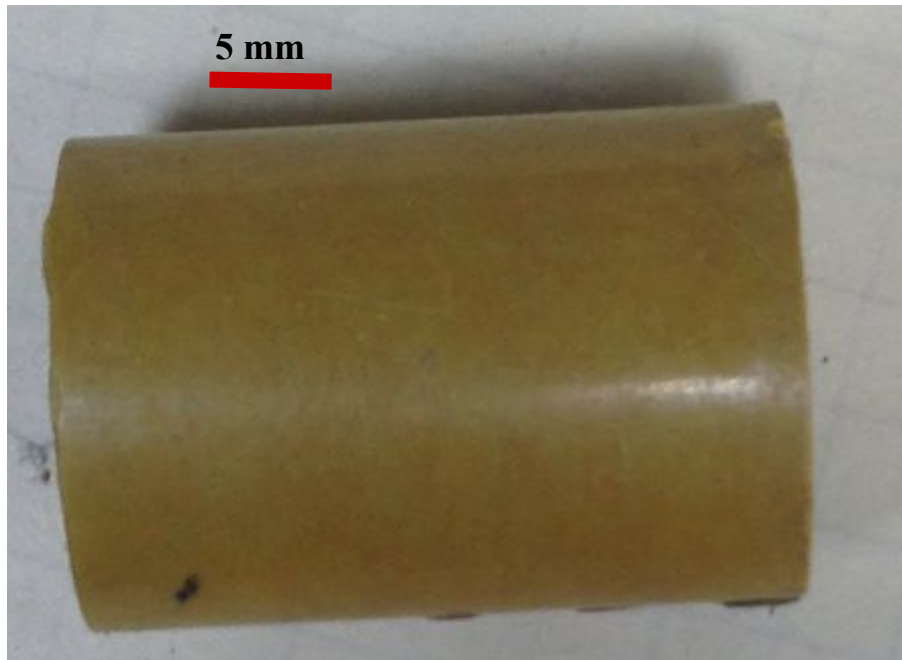
3. CsI:Tl films for X-ray Imaging

The tomography of dense objects using monochromatic and polychromatic X-ray beams



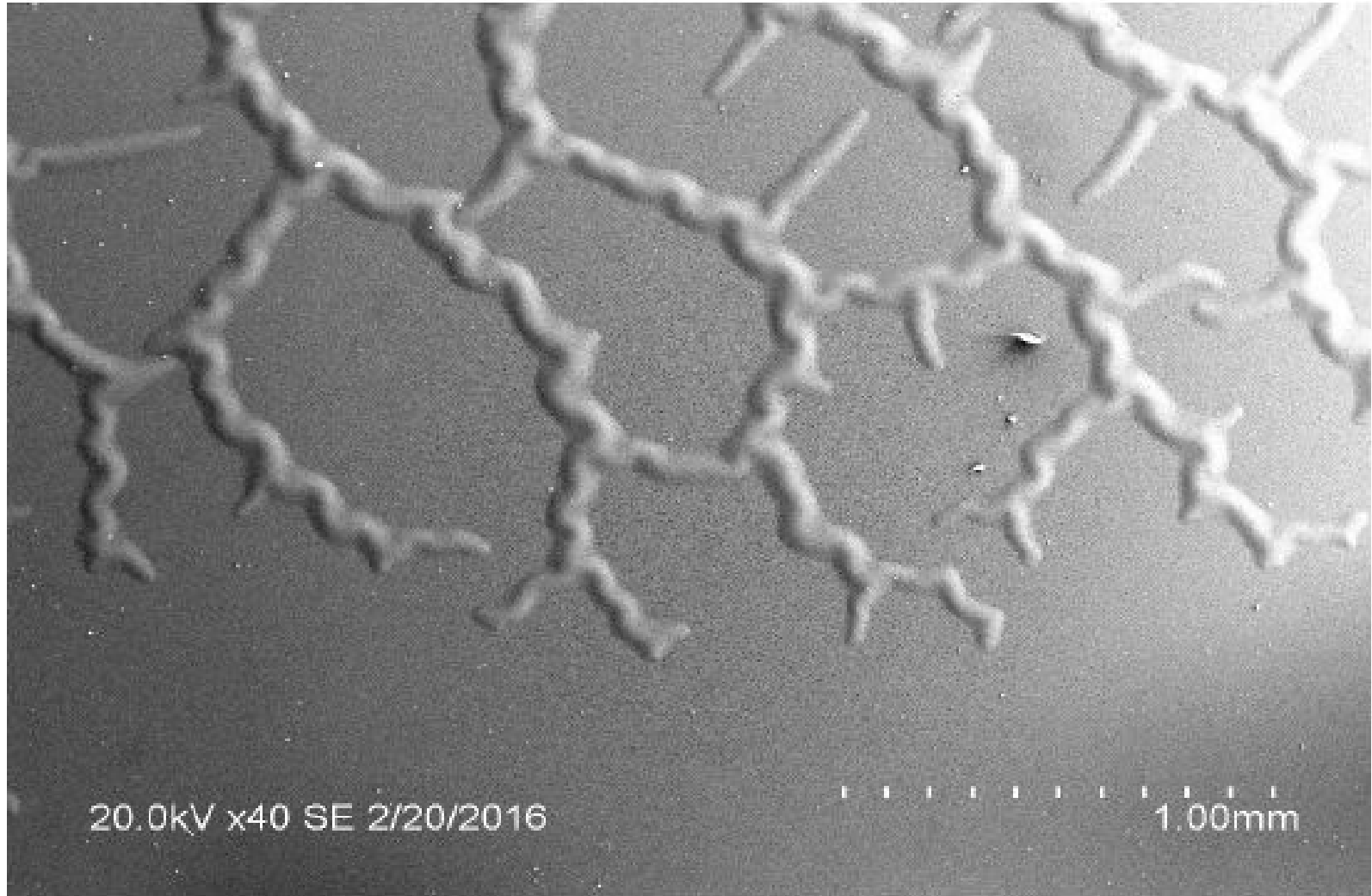
3. CsI:Tl films for X-ray Imaging

The tomography of dense objects using monochromatic and polychromatic X-ray beams



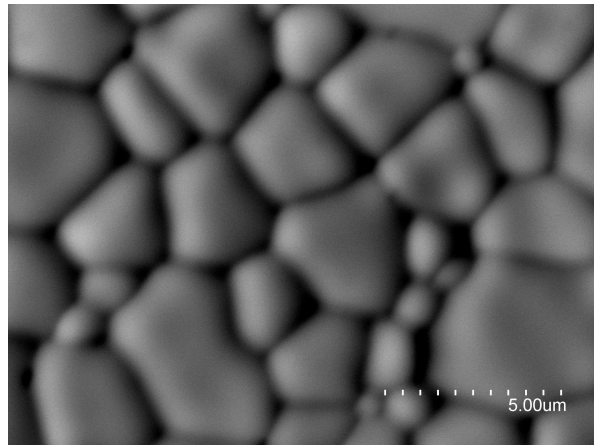
3. CsI:Tl films for X-ray Imaging

Destruction scintillator surface caused by ozone produced by interaction polychromatic SR with air.



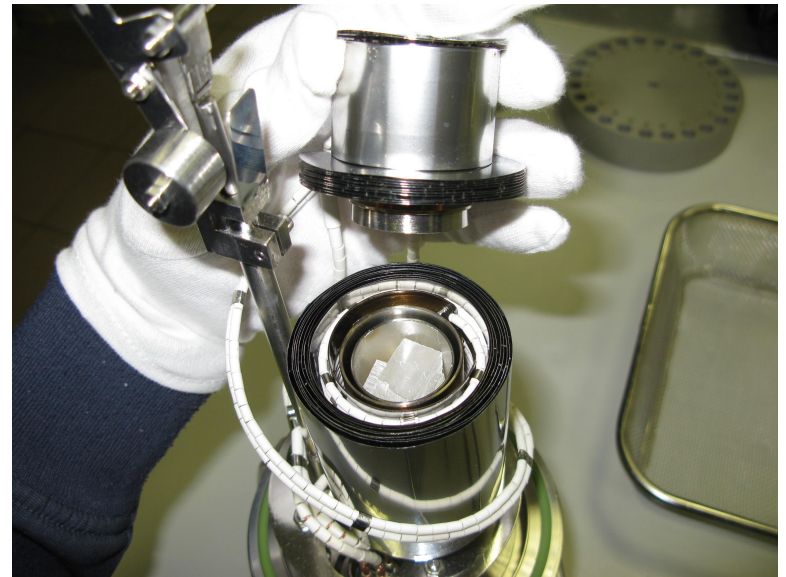
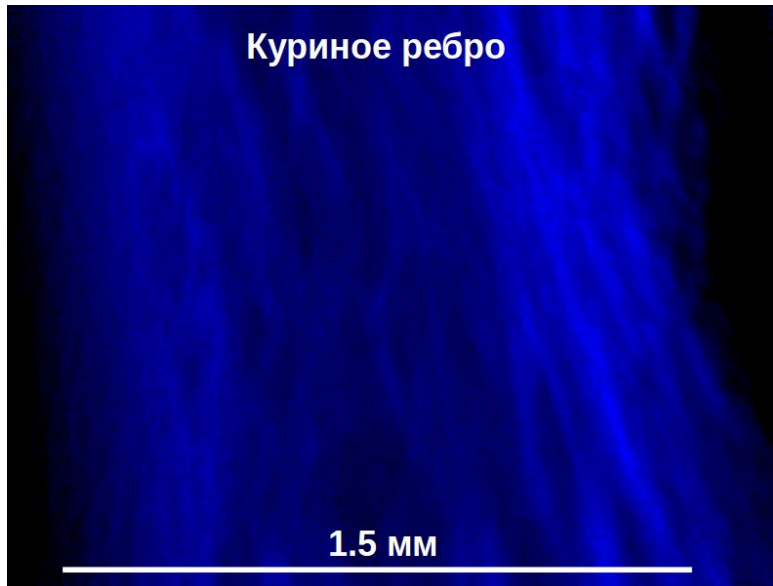
4. Conclusion

- **The methodics of performance of thin CsI:Tl films was developed.**
- **The relationship between the morphology of deposited layers and the characterization of the film was presented.**
- **The post-deposition treatment by carbon leads to significant improvement of spatial resolution.**
- **All X-ray radiographic methods can be employed with the films in polychromatic and monochromatic modes from 10 mkm of biological tissue up to 5 cm of dense rock.**



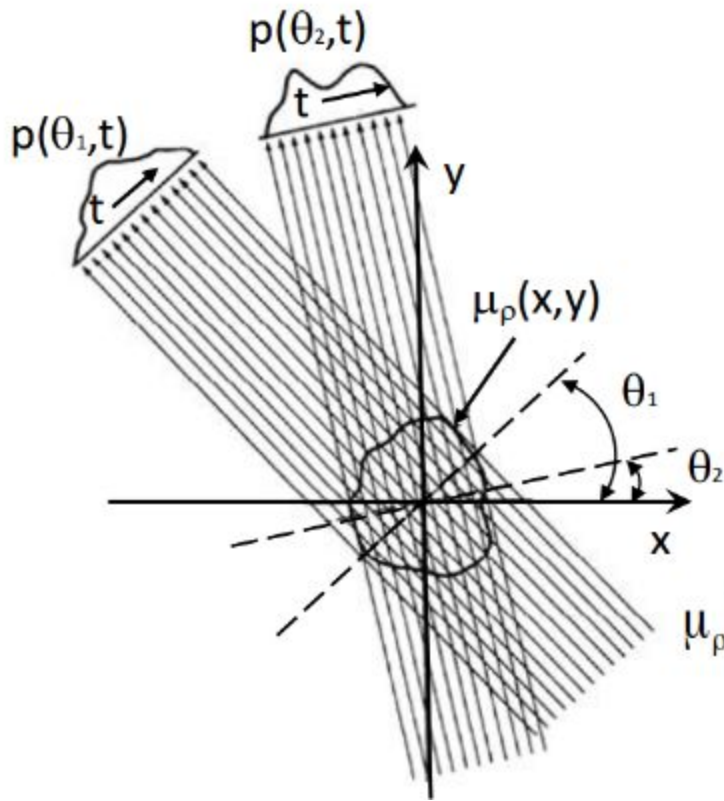
Thank you for your attention!

If you are interesting in precise imaging we are open for interaction.



Компьютерная томография

Набор проекционных данных, получаемых при вращении образца



$$p(t, \theta_1) = \int_L \mu_\rho(t, s) ds$$

$$p(t, \theta_2) = \int_L \mu_\rho(t, s) ds$$

.....

$$p(t, \theta_n) = \int_L \mu_\rho(t, s) ds$$

Набор проекционных данных, где $\mu_\rho = \mu \cdot \rho$ - удельный коэффициент поглощения рентгеновского излучения.



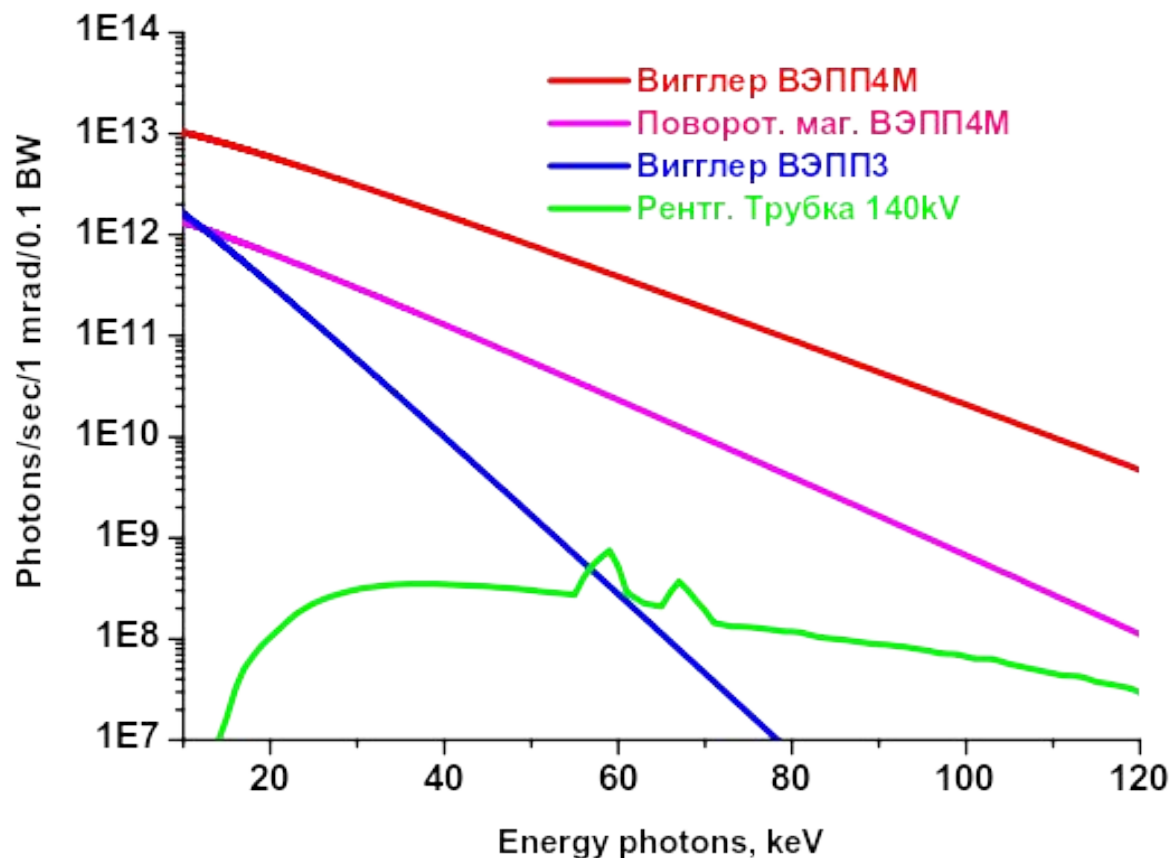
Теорема о центральном сечении

Фурье-образ $P(\omega, \theta) = F(\omega \cdot \cos\theta, \omega \cdot \sin\theta)$, где F — Фурье-образ μ



$$\mu_\rho(x, y) = \frac{1}{4\pi^2} \iint \omega P(\omega, \theta) e^{i\omega(x \cos\theta + y \sin\theta)} d\omega d\theta$$

Источники СИ в ИЯФ СО РАН



Широкий энергетический спектр **[5-100] кэВ** позволяет диагностировать объекты разной толщины, начиная от **~ 10 мкм биологической ткани** и заканчивая **~ 5 см горной породы**.

Источники СИ в ИЯФ СО РАН

Инжектор:

1 — Гиротрон (430 МГц)

2 — Линейный ускоритель (50 МэВ)

3 — Электрон-позитронный конвертер

4 — Синхротрон Б-4 (350 МэВ)

